Pharm Res (2014) 31:1978–1988
DOI 10.1007/s11095-014-1300-z

RESEARCH PAPER

Development of Vorinostat-Loaded Solid Lipid Nanoparticles to Enhance Pharmacokinetics and Efficacy against Multidrug-Resistant Cancer Cells

Tuan Hiep Tran • Thiruganesh Ramasamy • Duy Hieu Truong • Beom Soo Shin • Han-Gon Choi • Chul Soon Yong • Jong Oh Kim

Received: 27 October 2013 / Accepted: 14 January 2014 / Published online: 22 February 2014

ABSTRACT

Purpose To investigate whether delivery of a histone deacetylase inhibitor, vorinostat (VOR), by using solid lipid nanoparticles (SLNs) enhanced its bioavailability and effects on multidrug-resistant cancer cells.

Methods VOR-loaded SLNs (VOR-SLNs) were prepared by hot homogenization using an emulsification-sonication technique, and the formulation parameters were optimized. The cytotoxicity of the optimized formulation was evaluated in cancer cell lines (MCF-7, A549, and MDA-MB-231), and pharmacokinetic parameters were examined following oral and intravenous (IV) administration to rats.

Results VOR-SLNs were spherical, with a narrowly distributed average size of ~100 nm, and were physically stable for 3 months. Drug release showed a typical bi-phasic pattern *in vitro*, and was independent of pH. VOR-SLNs were more cytotoxic than the free drug in both sensitive (MCF-7 and A549) and resistant (MDA-MB-231) cancer cells. Importantly, SLN formulations showed prominent cytotoxicity in MDA-MB-231 cells at low doses, suggesting an ability to effectively counter the P-glycoprotein-related drug efflux pumps. Pharmacokinetic studies clearly demonstrated that VOR-SLNs markedly improved VOR plasma circulation time and decreased its elimination rate constant. The areas under the VOR concentration-time curve produced by oral and IV administration of VOR-SLNs were significantly greater than those produced by free drug administration. These *in vivo* results clearly highlighted the remarkable potential of SLNs to augment the bioavailability of VOR.

Conclusions VOR-SLNs successfully enhanced the oral bioavailability, circulation half-life, and chemotherapeutic potential of VOR.

KEY WORDS Bioavailability · Drug resistance · Pharmacokinetics · Solid lipid nanoparticle · Vorinostat

INTRODUCTION

Vorinostat (VOR) is a histone deacetylase inhibitor that can effectively induce cell cycle arrest, cell differentiation, and apoptosis (1). It has been approved by the FDA for the treatment of cutaneous T-cell lymphoma (CTCL) (2, 3). The clinical efficacy of VOR has also been investigated in other solid malignancies, leukemia, and various autoimmune disorders (4). Despite showing such chemotherapeutic promise, the clinical efficacy of VOR has been limited by its poor aqueous solubility (0.2 mg/mL) and low permeability (a log partition coefficient of 1.9), leading to its assignment to class IV of the Biopharmaceutics Classification System (BCS) (5). These suboptimal parameters limited the absolute bioavailability (F) of this drug in the systemic circulation, necessitating either a higher oral dose or a higher frequency of administration (6). In addition to these poor physicochemical properties, oral delivery of anti-cancer drugs needs to overcome physiological barriers, such as pre-systemic metabolism and gastrointestinal instability, to achieve high therapeutic efficacy (7). Extensive first-pass metabolism of VOR (49 to 75 L/h/m^2) has been reported in both animal and human studies (7, 8). VOR is metabolized via two metabolic pathways involving glucuronidation and hydrolysis, followed by β-

T. H. Tran • T. Ramasamy • D. H. Truong • C. S. Yong (✉) • J. O. Kim (✉)
College of Pharmacy, Yeungnam University
214-1, Dae-Dong Gyeongsan 712-749, South Korea
e-mail: csyong@ynu.ac.kr
e-mail: jongohkim@yu.ac.kr

B. S. Shin
College of Pharmacy, Catholic University of Daegu
Gyeongsan 712-702, South Korea

H.-G. Choi
College of Pharmacy, Hanyang University
55, Hanyangdaehak-ro, Sangnok-gu Ansan
426-791, South Korea

oxidation. It is mainly metabolized in the liver, with some kidney involvement (5).

Although parenteral administration of VOR might be predicted to overcome some of these barriers, it has also resulted in a poor pharmacokinetic response. VOR exhibited a short half-life of 40 min following intravenous (IV) administration (compared with ~2 h following oral administration). Furthermore, the limited aqueous solubility of VOR could result in the formation of aggregates in the plasma after IV administration that would cause embolization before reaching the tumor target (9). To overcome these drawbacks, various strategies have been attempted, such as incorporation of VOR into micelle nanocarriers (5), inclusion cyclodextrins (2), and silicon microstructures (10). However, none of these approaches has improved the physicochemical or pharmacological properties of this drug to a satisfactory level. There is therefore a need for a simple, stable, and effective delivery system that can provide clinically viable oral and IV administration of VOR.

Solid lipid nanoparticles (SLNs) are one of the most sought-after colloidal nanocarrier systems for the delivery of anti-cancer drugs (11). The physiological lipid core within SLNs can protect labile compounds from chemical degradation and improve their stability (12). SLNs improve the oral bioavailability of BCS class IV drugs by avoiding first-pass metabolism and bypassing the efflux transporters because of the presence of long-chain fatty acids (13). In addition, SLNs have been demonstrated to overcome multidrug resistance (MDR), modulate release kinetics, improve blood circulation time, and increase overall therapeutic efficacy of anti-cancer drugs (14, 15).

To investigate whether SLNs could potentially provide a clinically useful VOR delivery system for cancer treatment, VOR-loaded SLNs (VOR-SLNs) were formulated. We postulated that VOR-SLNs could improve the oral bioavailability, plasma stability, and systemic half-life of the drug, as well as improve efficacy against multidrug-resistant cancer cells. These features would all contribute to improving the antitumor efficacy of VOR. This hypothesis was tested *in vitro* and *in vivo* by quantifying VOR-SLNs cytotoxicity against drug-sensitive and drug-resistant cancer cell lines (A-549, MCF-7, and MDA-MB-231), and by administering VOR-SLNs orally and IV to rats, enabling assessment of pharmacokinetics. Importantly, assessing the *in vivo* pharmacokinetics via two routes produced data that could facilitate the development of formulations for both oral and parenteral use.

MATERIALS AND METHODS

Materials

VOR was purchased from LC laboratories (MA, USA). Compritol 888 ATO (powder state; melting point, 70°C) was procured from Gattefosse (Cedex, France). Soybean lecithin was purchased from Junsei Co. Ltd (Tokyo, Japan). 3-(4,5-Dimethylthiazol-2-yl)-2,5-diphenyl-tetrazolium bromide (MTT) was obtained from Sigma (St. Louis, MO, USA). The MCF-7, MDA-MB-231, and A-549 cells were originally obtained from the Korean Cell Line Bank (Seoul, South Korea). All other chemicals were of reagent grade and were used without further purification.

Preparation of VOR-Loaded SLNs

VOR-SLNs were prepared by the hot homogenization method using an emulsification-sonication technique (16, 17). Based on a preliminary analysis of potential lipids and surfactants (data not shown), Compritol 888 ATO, lecithin, and Tween 80 were selected for preparation of SLNs. Briefly, the lipid phase was prepared by melting Compritol 888 ATO, lecithin, and VOR at 10°C above the lipid melting point to obtain a clear transparent solution. The aqueous phase was prepared by dissolving Tween 80 in distilled water and heating to the final temperature of the lipid phase. Next, the hot aqueous phase was gently added drop-wise into the lipid phase with constant stirring at 13,500 rpm in an Ultra Turrax® T-25 homogenizer (IKA®-Werke, Staufen, Germany) for 3 min. The resulting coarse emulsion was immediately sonicated using a high-intensity probe sonicator (Vibracell VCX130; Sonics, USA) at 80% amplitude for 10 min. The resulting suspension was then cooled in an ice bath. The free drug was then removed by washing three times by using an ultracentrifugal device (Amicon Ultra, Millipore, USA). The particles retained inside the device were dispersed in distilled water and used in subsequent experiments. The various compositions of SLNs are given in Table I.

Lyophilization of SLNs

The SLN dispersion was lyophilized using trehalose as a cryoprotectant (FDA5518, IlShin, South Korea). The dispersion was pre-frozen (−80°C) for 12 h and subsequently lyophilized at a temperature of −25°C for 24 h, followed by a secondary drying phase for 12 h at 20°C.

Measurement of Particle Size and ζ-potential

The SLN dispersions were diluted to an appropriate concentration in distilled water prior to measurement of mean particle diameter, polydispersity index (PDI), and ζ-potential by the dynamic light scattering (DLS) technique using a Zetasizer Nano–Z (Malvern Instruments, Worcestershire, UK) at a fixed scattering angle of 90° and at a temperature of 25°C. The data were determined using the Nano DTS software (version 6.34) provided by the manufacturers. All measurements were performed in triplicate.

Table I Composition of VOR SLNs

Formulations	Lecithin (g)	Tween 80 (g)	Vorinostat (g)	Compritol (g)	Distilled water (mL)
F1	0.10	0.10	–	0.5	15
F2	0.25	0.25	–	0.5	15
F3	0.30	0.30	–	0.5	15
F4	0.40	0.40	–	0.5	15
F5	0.50	0.50	–	0.5	15
F6	0.75	0.75	–	0.5	15
F7	0.20	0.80	–	0.5	15
F8	0.25	0.75	–	0.5	15
F9	0.33	0.67	–	0.5	15
F10	0.50	0.50	–	0.5	15
F11	0.67	0.33	–	0.5	15
F12	0.75	0.25	–	0.5	15
F13	0.80	0.20	–	0.5	15
F14	0.50	0.50	0.005	0.5	15
F15	0.50	0.50	0.010	0.5	15
F16	0.50	0.50	0.015	0.5	15
F17	0.50	0.50	0.020	0.5	15
F18	0.50	0.50	0.025	0.5	15

Determination of Drug Encapsulation Efficiency

The encapsulation efficiency (EE) of VOR in SLNs was determined by ultrafiltration using centrifugal devices (Amicon Ultra, Millipore, USA) with a 10-kDa molecular weight cut-off membrane (18). In order to quantify un-encapsulated VOR in the SLN dispersions, an aliquot (2 mL) of VOR-SLNs was placed in a centrifugal filter tube and centrifuged (10 min at 5,000 rpm) to separate free drug from encapsulated drug. The filtrate was then diluted in acetonitrile and analyzed for VOR using high-performance liquid chromatography (HPLC). Formic acid (0.1%)/acetonitrile (60/40) was used as a mobile phase at a flow rate of 1.0 mL/min. VOR was detected at 241 nm. The EE and drug loading capacity (LC) were calculated using the following equations:

$$EE\% = \frac{M_{drug\ in\ SLN}}{M_{initial\ drug}} \times 100 \quad LC\% = \frac{M_{drug\ in\ SLN}}{M_{SLN}} \times 100$$

where $M_{drug\ in\ SLN}$ was the amount of VOR incorporated in SLN, $M_{initial\ drug}$ was the amount of VOR added initially, and M_{SLN} was the total amount of SLN.

Morphological Analysis

Morphological examination of SLNs was performed using a transmission electron microscope (TEM; H7600, Hitachi, Tokyo, Japan) at an accelerating voltage of 100 kV. The samples were stained with 2% (w/v) phosphotungstic acid and placed on a copper grid, followed by gentle drying.

Solid-State Characterization of VOR-SLNs

Differential scanning calorimetry (DSC) analysis was performed using a DSC-Q200 differential scanning calorimeter (TA Instruments, New Castle, DE, USA). Freeze-dried SLNs were put into mini-aluminum pans and the temperature was increased from 40 to 180°C at a rate of 10°C/min under a dynamic nitrogen atmosphere with flow rate of 50 mL/min. An empty pan was used as a reference before commencement of the sample run. In addition, crystalline structures of the lyophilized SLNs were investigated using an X-ray diffractometer (X'Pert PRO MPD diffractometer, Almelo, The Netherlands) with a copper anode (Cu Kα radiation, 40 kV, 30 mA, $\lambda = 0.15418$). The data were typically collected with a step width of 0.04° and a detector resolution of 2θ (diffraction angle) between 10°C and 60°C.

In Vitro Drug Release Study

The release of VOR from the optimized VOR-SLNs (~80 nm, ~0.2 PDI) was evaluated by dialysis in media with a range of pH values (pH 1.2, 5.0, 6.8, and 7.4) by using membrane tubing with a 3,500 Da cut-off (Spectra/Por®, CA, USA). The experiment was performed at 37°C with a shaking speed of 100 rpm. Medium samples (0.5 mL) were collected at various time points and replaced with 0.5 mL of fresh medium. The concentrations of VOR released from the SLNs into the media were measured using the HPLC system described above.

Stability Studies

The storage stability of VOR-SLNs (lyophilized and dispersion form) was assessed for 3 months under two different conditions: at 4°C and at ambient room temperature (25°C). The stability of VOR-SLNs was assessed in terms of particle size, PD, ζ-potential, and drug content (%)

In Vitro Cytotoxicity Assay

The *in vitro* cytotoxicity of blank SLNs, free VOR, and VOR-SLNs was evaluated against two human breast cancer cell lines (MCF-7 and MDA-MB-231) and a human non-small cell lung cancer cell (A-549) by using the MTT assay as reported previously (19). The cell lines were routinely cultured in RPMI-1640 supplemented with 10% fetal bovine serum (FBS) and 1% penicillin/streptomycin, incubated at 37°C in a 5% CO_2 humidified incubator. For the experiments, 100 μL of cell suspension was seeded in a 96-well plate at a density of 5×10^3 cells/well, and incubated for 24 h. A concentration

range of blank SLNs, free VOR, and VOR-SLNs was added to each well plate and incubated for 24 or 48 h. The cells were then washed twice with phosphate-buffered saline. MTT solution (100 μL of 1.25 mg/mL) was added to each well and the plate was placed in an incubator for 3 h at 37°C in the dark. The cells were then treated with 100 μL of DMSO and the absorbance was measured at 570 nm by using a microplate reader (Multiskan EX, Thermo Scientific, Waltham, MA, USA). Cell viability was calculated using the following formula:

$$\text{Cell viability } (\%) = \frac{OD_{570}(\text{sample}) - OD_{570}(\text{blank})}{OD_{570}(\text{control}) - OD_{570}(\text{blank})} \times 100$$

Pharmacokinetic Study

Male Sprague–Dawley rats weighing 250 ± 10 g were divided into 4 groups of 4 rats. The animals were quarantined in an animal house maintained at 20 ± 2°C and 50–60% RH, and fasted for 12 h prior to the experiments. The protocols for the animal studies were approved by the Institutional Animal Ethical Committee, Yeungnam University, South Korea.

Two groups of rats received free VOR (one group orally, one group IV) and the other two groups received VOR-SLNs (one group orally, one group IV). Free VOR was dispersed in 1% methylcellulose for oral administration at a dose of 30 mg/kg of body weight. For IV injection, VOR was dissolved in 10% PEG 400 (in which the drug was completely soluble) and administered at a dose of 10 mg/kg. The difference in oral and IV dosage was because of the low bioavailability of orally administered VOR. Blood samples (300 μL) were collected from the right femoral artery at predetermined times (0.25, 0.5, 1, 2, 3, 4, 6, 8, 12, and 24 h) after administration of these formulations. The samples were collected in heparin-containing tubes (100 IU/mL) and then immediately centrifuged (Eppendorf, Hauppauge, NY, USA) at 14,000 rpm for 10 min. The plasma supernatant was collected and stored at −20°C until further analysis.

Plasma Sample Processing

To extract VOR and to precipitate unwanted protein, 150 μL of plasma was mixed with 150 μL of acetonitrile for 30 min. The samples were then centrifuged at 14,000 rpm for 10 min and 20 μL of the supernatant was injected into the HPLC system for VOR analysis, described above.

Analysis of Pharmacokinetic Data

The pharmacokinetic profiles of free VOR and VOR-SLNs were calculated using the Win-NonLin pharmacokinetic software (v 4.0, Pharsight Software, Mountain View, CA, USA). The pharmacokinetic data measured included the area under the plasma drug concentration–time curves from time zero to infinity ($AUC_{0-\infty}$), the half-life of elimination ($t_{1/2}$), and the clearance (Cl). The Cl value was calculated as the dose/$AUC_{0-\infty}$, and the mean residence time (MRT) was obtained by summation of the central and tissue compartments.

Statistical Analysis

Analysis of variance (ANOVA) was performed to investigate differences between the experimental treatments. A p-value of <0.05 was considered statistically significant in all cases, and all data were expressed as mean±standard deviation.

RESULTS

Preparation of VOR-SLNs

The effects of various formulation variables (lecithin, Tween 80, and VOR) were investigated to obtain a narrowly distributed SLN with high drug entrapment efficiency (Fig. 1). Table I summarizes the composition of the blank SLNs and VOR-SLNs. As can be seen in Fig. 1a, hydrodynamic particle size decreased with increasing surfactant concentration (F1-F6), whereas particle size increased as lecithin concentration increased (F7-F13, Fig. 1b). The surfactant-related decrease in size is consistent with the general perception that a higher concentration of surfactant would completely cover the SLN surface, while the increase in PDI may result from the random formation of SLNs of different sizes. Furthermore, an increased level of amphiphilic surfactant at the outer surface (F6) may reduce overall surface charge. Meanwhile, SLN size was unaffected by VOR concentration (F14-F18, Fig. 1c). The optimized formulation (F17) had the smallest size (86.5 ± 4.5 nm), acceptable polydispersity (0.289 ± 0.01), and ζ-potential (−22.2 ± 0.5 mV). VOR-SLNs showed high EE (~70%), indicating successful drug entrapment within the core (Table II). TEM indicated a spherical SLN morphology with a size largely consistent with the DLS characterization results (Fig. 2). These analyses indicated that VOR-SLNs were nanometer sized with a well-dispersed pattern.

Solid-State Characterization

The thermal behaviors of the optimized formulation (F17) were investigated to monitor the physical and chemical changes within the sample (Fig. 3). Free VOR and Compritol showed sharp endothermic peaks at around 163°C and 73°C, respectively, corresponding to the melting points of their crystalline forms. The absence of a comparable endothermic peak from VOR-SLNs indicated that the drug was in

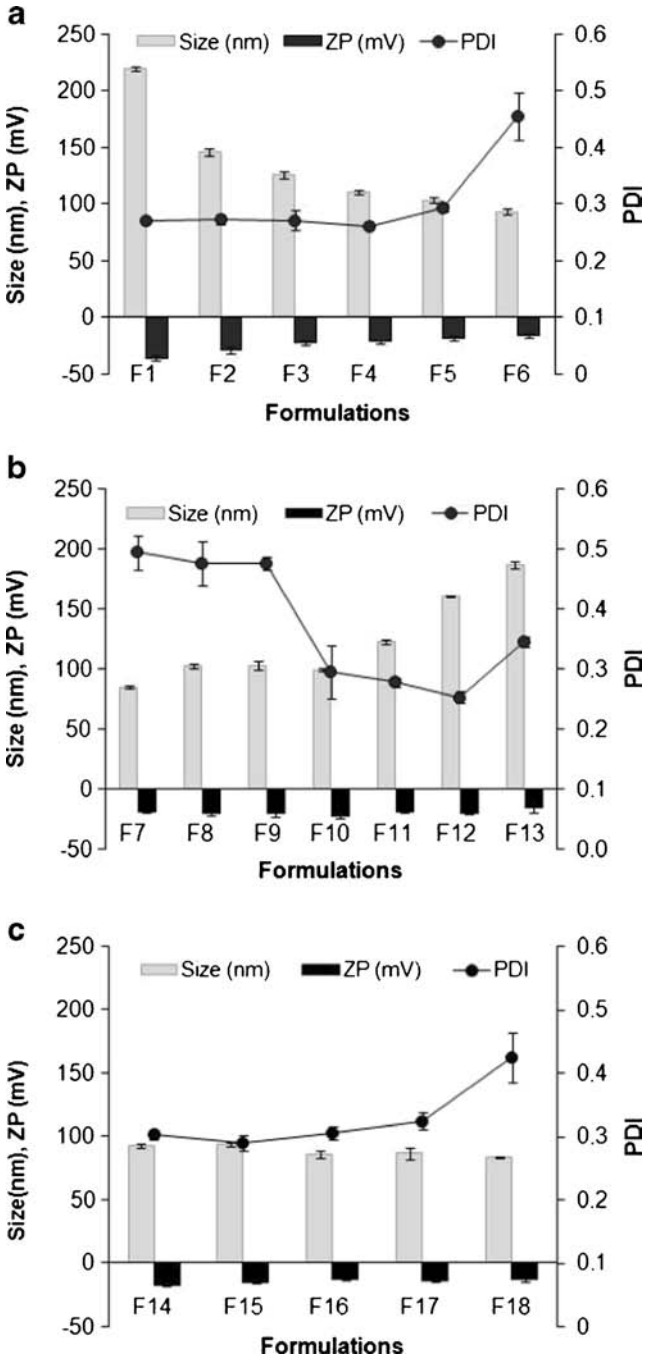

Fig. 1 Effect of SLN composition on particle size, polydispersity index (PDI) and ζ-potential. (**a**) Effect of the amount of surfactant, using a constant lecithin:Tween 80 ratio. (**b**) Effect of the lecithin:Tween 80 ratio, using a constant amount of surfactant. (**c**) Effect of the amount of VOR, using the optimal SLN formulation. ZP: ζ-potential. Data represent the mean ± standard deviation ($n = 3$).

an amorphous state after successful encapsulation into the SLN. Instead, a small peak was observed at 68°C, corresponding to the melting point of Compritol. These finding were confirmed by the XRD patterns produced by Compritol, free VOR, and VOR-SLNs. As can be seen in Fig. 3b, VOR showed numerous diffraction peaks at several 2θ scattered angles owing to its crystalline nature, while no such peaks were observed in VOR-SLNs. This observation clearly suggested that VOR was amorphous within the crystal lattice of the SLN lipid matrix, in agreement with the DSC data.

Table II Drug encapsulation efficiency (EE) and drug loading capacity (LC) of VOR-SLNs. Data are expressed as the mean ± standard deviation ($n = 3$)

Formulations	EE (%)	LC (%)
F14	70.19 ± 1.02	0.69 ± 0.01
F15	66.21 ± 0.49	1.29 ± 0.12
F16	66.98 ± 0.52	1.95 ± 0.09
F17	69.43 ± 0.92	2.67 ± 0.08
F18	63.47 ± 0.34	3.02 ± 0.21

Stability

Table III shows the changes in physical properties over time when the VOR-SLNs were stored under different conditions. After 3 months at room temperature, particle size, PDI, and ζ-potential of VOR-SLNs had slightly increased, while drug content (%) had slightly decreased. In contrast, there was no change when VOR-SLNs were stored at 4°C or freeze-dried, which indicated that this formulation was physically stable under these storage conditions.

In Vitro Drug Release

In vitro release profiles of VOR-SLNs are presented in Fig. 4. VOR-SLNs exhibited a bi-phasic release pattern with an initial burst release of 25% of the drug within the first 2 h of the study period, followed by a sustained release of up to 35% within 24 h. It is worth noting that the release pattern was the same, regardless of dissolution media pH.

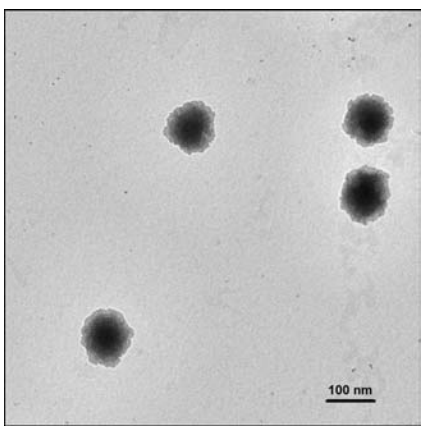

Fig. 2 TEM image of VOR-SLNs.

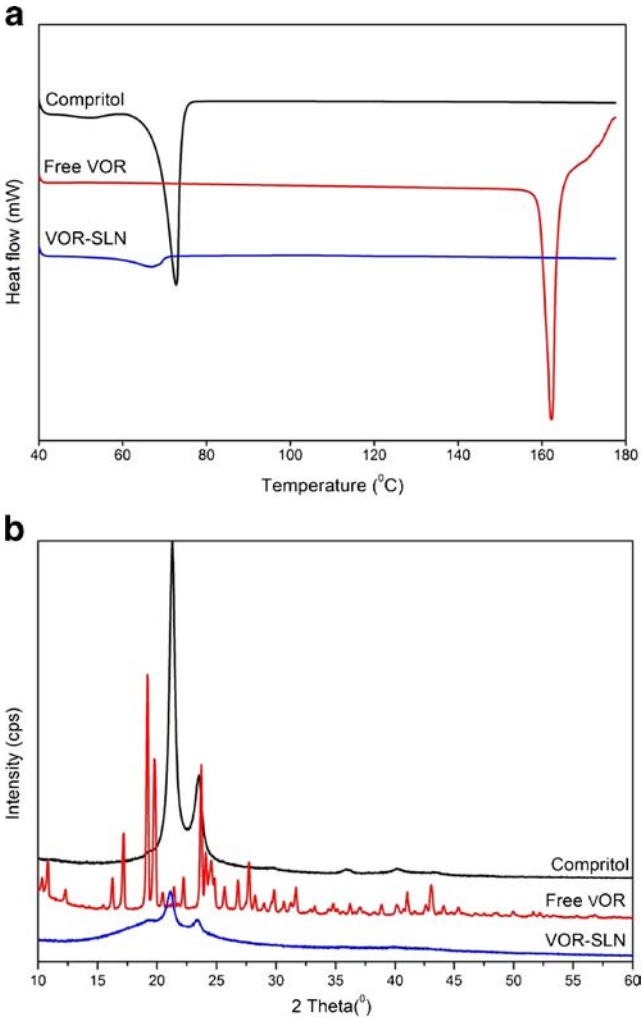

Fig. 3 (**a**) Differential scanning calorimetric (DSC) thermograms and (**b**) X-ray diffraction (XRD) patterns of free VOR and VOR-SLNs.

In Vitro Cytotoxicity

The cytotoxicity of blank SLNs, free VOR, and VOR-SLNs was evaluated in MCF-7, A-549, and MDA-MB-231 cells (Fig. 5). Blank SLNs did not exhibit any appreciable cytotoxicity and the cell viability remained more than 80% in all the cell lines following 24-h exposure to the tested concentration range of 0.5–50 μg/mL. Similar observations were noted even when cells were exposed to the blank SLNs for 48 h, suggesting excellent cytocompatibility of the SLN system. VOR-SLNs were found to significantly suppress cell proliferation in a dose- and time-dependent manner. The cytotoxicity of VOR-SLNs was significantly higher than that of free VOR in all the cell lines tested. Notably, VOR-SLNs showed more prominent inhibitory effects than free VOR in both sensitive cells (MCF-7 and A-549) and drug-resistant cells (MDA-MB-231).

Pharmacokinetic Study

The plasma concentration-time profiles of free VOR and VOR-SLNs after oral and IV administration are shown in Fig. 6. The oral dose of VOR was 30 mg/kg, compared to 10 mg/kg IV, because lower oral VOR doses produced undetectable plasma VOR levels, due to its low oral absorption rate. As can be seen, the mean plasma concentration of VOR was much higher in the rats treated with oral VOR-SLNs than in the rats treated with oral free VOR at every time point following administration. Similar results were observed for IV administration. The rates and extent of drug absorption are summarized in Table IV. The C_{max} of VOR in the rats treated with oral VOR-SLNs (13.85 ± 3.02 μg/mL) was 1.6-fold higher than the C_{max} in the rats treated with oral free VOR (8.95 ± 0.12 μg/mL) ($p<0.05$). Most importantly, the $AUC_{0-\infty}$ of VOR-SLNs was 2.5-fold higher than that of the free VOR suspension ($p<0.05$), suggesting that SLN greatly improved the oral bioavailability profile of VOR and overcame many barriers limiting its systemic availability. In addition, the $t_{1/2}$ of VOR administered in the SLN formulation (4.9 h) was more than double than that observed following administration of the free VOR suspension (2.3 h). When administered via the IV route, VOR-SLNs exhibited a 7-fold higher $t_{1/2}$ and the $AUC_{0-\infty}$ was 2.7-fold greater than that achieved by free VOR. Similarly, the MRT produced by VOR-SLNs was markedly higher than that observed following free drug administration by oral or IV routes. These results clearly indicated that use of VOR-SLNs significantly augmented the oral bioavailability of VOR and resulted in a longer blood circulation time.

Table III Stability of formulations under different conditions. Data are expressed as the mean ± standard deviation ($n=3$)

Conditions	VOR-SLNs (F17)			
	Size (nm)	PDI	ZP (mV)	Drug content (%)
Initial	86.5 ± 4.5	0.289 ± 0.010	−22.2 ± 0.5	100.0 ± 0.92
3 months at 4°C	91.6 ± 3.2	0.297 ± 0.008	−21.6 ± 1.8	98.5 ± 1.32
3 months at 25°C	99.8 ± 4.3	0.305 ± 0.007	−18.4 ± 2.5	96.6 ± 2.14
After lyophilization	87.4 ± 2.9	0.286 ± 0.010	−22.9 ± 2.8	99.4 ± 1.1

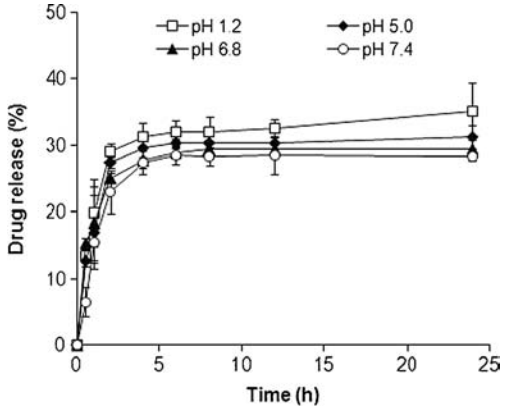

Fig. 4 *In vitro* drug release from VOR-SLNs under different conditions: pH 1.2 (□), pH 5.0 (◆), pH 6.8 (▲), and pH 7.4 (○). Data are expressed as the mean±standard deviation ($n=3$).

DISCUSSION

VOR is a class I and II histone deacetylase inhibitor that has proven efficacy against various solid tumors. Numerous *in vitro* and animal studies have demonstrated that VOR induced differentiation and apoptosis, inhibited cell proliferation, and exerted immune stimulatory and antiangiogenic activities (20, 21). In the clinical setting, VOR has been approved for the treatment of cutaneous T-cell lymphoma (22, 23). Despite its promising pharmacological effects, the clinical efficacy of VOR has been limited by poor aqueous solubility, low gastrointestinal (GI) permeability, extensive first-pass metabolism, and low therapeutic index (short $t_{1/2}$ and extensive clearance), all of which reduced its delivery to cancer cells (2, 24). To our knowledge, there have been no published reports of suitable drug delivery vehicles capable of improving these features of VOR. In this regard, SLNs offer an attractive means to deliver poorly water-soluble drugs such as VOR. SLNs consist of a biocompatible lipid core that can efficiently entrap the lipophilic drug and improve its physical and biological stability (24). SLNs have previously been reported to augment the pharmacokinetic profiles and targeting of anticancer drugs, while minimizing their systemic side effects (25). Besides improving the anti-cancer response, SLNs were shown to overcome the multidrug resistance (MDR) in P-glycoprotein (P-gp) over-expressing cells, making this system even more attractive for cancer therapy (26).

The present study successfully incorporated VOR into the SLN core and characterized important physicochemical, pharmacological, and pharmacokinetic features of the resulting VOR-SLNs. The effects of lecithin and Tween 80 on the physicochemical properties of the SLNs were investigated in detail because size, shape, and surface characteristics of nanoparticles play a vital role in drug distribution in the systemic circulation. In particular, spherical particles with a size below 200 nm preferentially accumulated in tumor tissues owing to the enhanced permeability and retention (EPR) effect (27), and mixtures of two or more surfactants were reported to stabilize the dispersive system and reduce nanoparticle size (28, 29). The present study employed lecithin as a lipophilic emulsifier and Tween 80 as a hydrophilic emulsifier. The hydrodynamic size of SLN decreased significantly with increasing concentrations of both surfactants, whilst the particle size increased when the concentration of one of the

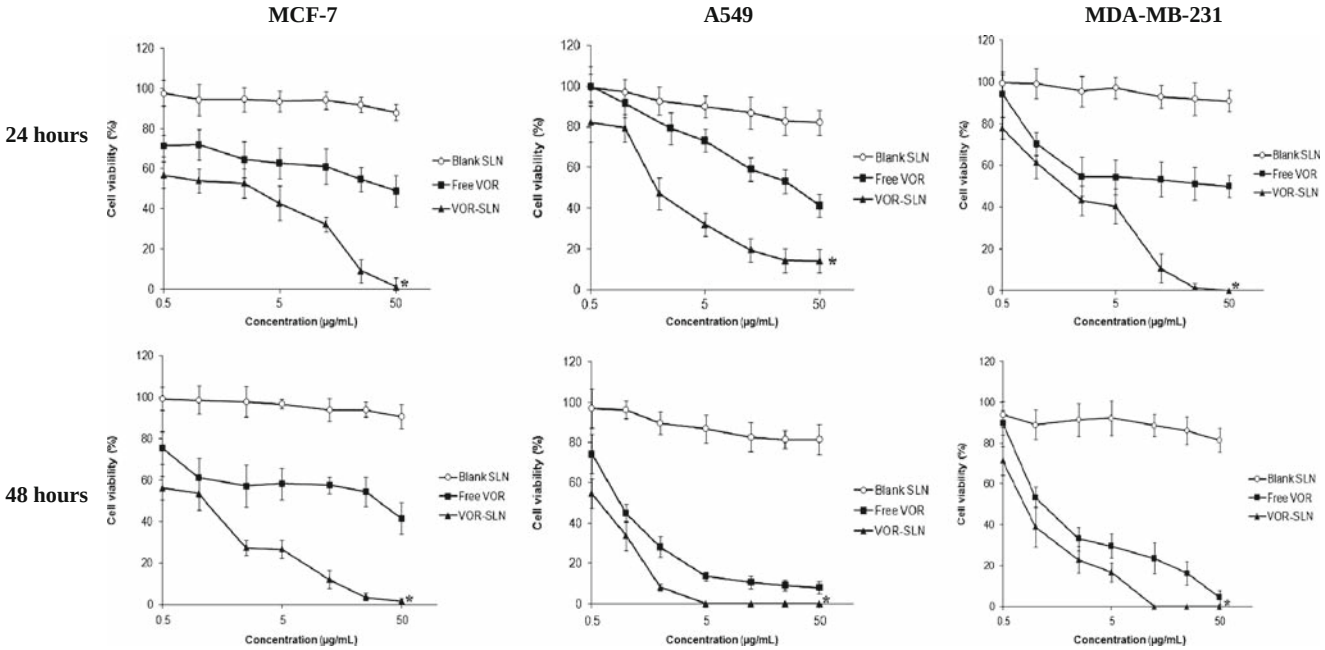

Fig. 5 Cell viability following exposure of MCF-7, A549, and MDA-MB-231 cells to blank SLNs, free VOR, and VOR-SLNs for 24 or 48 h. Data are expressed as the mean±standard deviation ($n=8$). * formulation induces significantly higher cytotoxicity ($p<0.05$) than free VOR does at all concentrations.

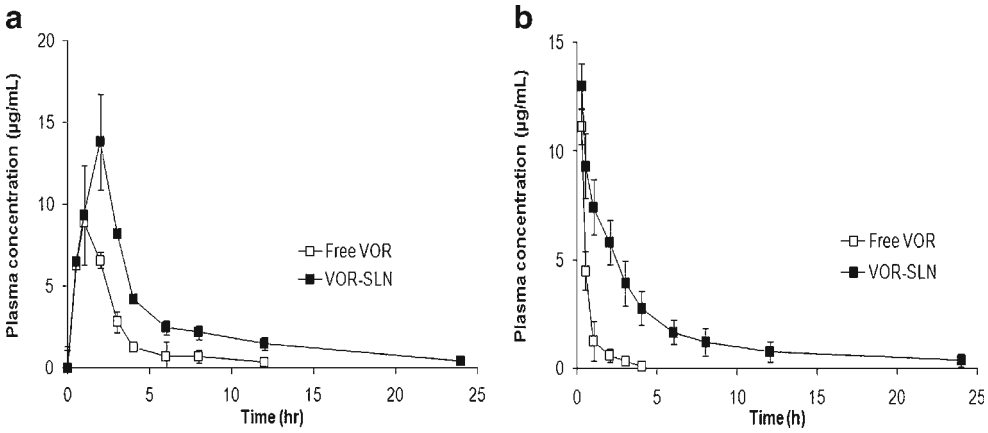

Fig. 6 Plasma concentration-time profile of VOR after (**a**) oral administration at a dose of 30 mg/kg and (**b**) IV administration at a dose of 10 mg/kg to rats of free VOR (□) or VOR-SLNs (■). Data are expressed as the mean ± standard deviation ($n=4$).

surfactants (Tween 80) was reduced. Notably, the particle size remained small when the ratio of lecithin to Tween 80 (0.2/0.8 = 0.25) was low, whereas the particle size increased dramatically when the ratio was higher (0.8/0.2 = 4). This might be because of the presence of Tween 80 (hydrophilic-lipophilic balance [HLB] = 15) on the outer layer of the SLN surface, whereas lecithin was preferably interspersed between the lipid layers. Use of lecithin alone as an emulsifier may not be sufficient to stabilize the SLN, owing to the difference between the HLB value of lecithin (HLB = 4) and the lipid core. The present study, and other previously published data, therefore, indicated that a combination of two emulsifiers with respective hydrophilic and lipophilic natures was recommended to obtain better stabilization of the dispersive system (28, 29). Generally, an increased surfactant level in the colloidal dispersions may lead to a reduced mean particle size, because of the surface-active properties of surfactants (30). However, when the radius of the curvature reaches a critical value, the surfactant no longer seems to energetically favor a further decrease in particle size. In this study, all the SLN formulations exhibited a uniformly dispersed size distribution (PDI, ~0.2). This could be due to the use of the high-pressure hot homogenization technique, as this produces small particle sizes. Consistent with a previous report (31), SLN particle size decreased dramatically during the hot homogenization process, and ensured nanoparticle homogeneity in this study.

TEM imaging and DLS characterization confirmed the generation of distinct and spherical SLNs, with a narrow size distribution. The surface charge of a nanoparticle is an important determinant of its physical and physiological stability in the blood. Nanoparticles with a strong positive surface charge encounter enhanced opsonin binding and recognition by the reticulo-endothelial system, resulting in faster clearance from the blood (27). Nanoparticulate delivery systems with a completely negative charge (≤ −30 mV) or a medium negative charge (~ −20 mV), combined with an appropriate steric structure related to the surfactant content, show improved physical and physiological stability in blood. These features enhance the half-life of the drug in circulation. VOR-SLNs possessed a surface charge sufficient to maintain stability for at least 3 months, which was likely because of the combination of electrostatic and steric stabilization of the surfactant mixture.

DSC was performed to analyze the state of VOR before and after SLN preparation, and these data clearly indicated that the VOR peak disappeared after the drug was loaded into SLNs. This might be attributed to complete miscibility of VOR with lipid, to transformation to an amorphous form, or to its complete entrapment within the lipid matrices, a prerequisite for sufficient EE. In addition, the observed shift in the melting point of Compritol from 73°C to 68°C may be attributed to the interaction of lipid with other SLN components during the preparation process. A less ordered crystal or amorphous lipid matrix would be favorable for encapsulating more amounts of the drug (27). The free VOR XRD peaks either were reduced in intensity or absent in VOR-SLN formulations, confirming the change of free crystalline VOR to an amorphous form in VOR-SLNs. In addition, weaker peaks at 21° and 24° corresponded to lipid peaks whose intensity was reduced in the formulations, indicating a decrease in the degree of crystallinity. This change in lipid and drug crystallinity may have affected the EE and release profile of VOR from SLN. The EE remained around 70% in formulations with a range of VOR concentrations. Although EE decreased slightly from 70% to 63% as VOR levels increased, there were no significant differences ($p<0.05$). This may have been because of the presence of less ordered lipids that could accommodate more drug molecules and limit drug expulsion (32). Similarly, high drug-loading capacities of SLNs have been reported previously by many authors (33, 34).

VOR-SLNs exhibited pH-independent and bi-phasic patterns of drug release under all the pH conditions tested. Around 30% of VOR was released in the first 4 h of dialysis, increasing to ~35% at 24 h. Such a sustained release indicated the presence of the drug deep inside the SLN physiological lipid core. In addition, these data showed that more than 65% of VOR was still available within the nanoparticulate system for delivery to the cancer cells via the EPR effect, provided the SLN achieved a long blood circulation time (35). Similar bi-

phasic release profiles with an initial burst followed by prolonged release from SLN prepared using the hot homogenization technique have been reported by other researchers (36–38). The initial burst release may be attributed to the drug-enriched shell model of VOR incorporation into the SLN carrier system. During the high-pressure hot homogenization process, active compound may partition from the more soluble lipid phase into the hot aqueous phase, leading to increased solubility in the aqueous phase. During the subsequent cooling step, the lipid matrix starts crystallizing while a significant proportion of the active compound is still concentrated in the aqueous phase. During the supersaturation step, active compound in the aqueous phase attempts to partition back into the lipid phase. Since a solid core has already formed or has started forming, these active molecules accumulate in the outer liquid shell, leading to the formation of a drug-enriched shell. Such shell-based drug is generally responsible for the initial burst of release, due to its short diffusion path to the release media (38–40).

The cytotoxic effects of free VOR and VOR-SLNs were investigated in sensitive (MCF-7 and A-549) and resistant (MDA-MB-231) cancer cell lines to investigate whether VOR-SLNs had superior anti-cancer effects. This study demonstrated that although free VOR and VOR-SLNs both exhibited dose-dependent cytotoxicity in all the cell lines, VOR-SLNs were significantly more cytotoxic than free VOR at 24 h. This superior cytotoxicity (lower IC_{50} values) was even more apparent following 48 h incubation. The enhanced cytotoxic effect of VOR-SLNs compared to free VOR may reflect the lipophilic nature of the carrier, facilitating intracellular uptake. One of the hallmarks of multidrug-resistant cells is the over-expression of the P-gp drug efflux pump, which confers resistance to a variety of drugs (41). In this regard, our most notable observation came from the MDA-MB-231 resistant cell data, where only 50% cell death occurred at the highest concentration of free VOR (50 μg/mL, 24 h), while none of the cells were viable following 24 h incubation with VOR-SLNs at the same concentration. Similar results were observed with the sensitive cell lines (MCF-7 and A-549). These results demonstrated for the first time that incorporation of VOR into a lipid nanocarrier could sensitize both drug-sensitive and drug-resistant cells to much lower doses of this cytotoxic agent, compared to free drug. VOR-SLNs possessed markedly increased solubility and dissolution rates, which may facilitate generation of a higher drug concentration around the cells and increase the anti-cancer effects. However, many reports have also suggested that SLNs could be non-specifically internalized into cells via endocytosis or phagocytosis (15, 42). The enhanced cellular uptake of VOR-SLNs may affect cell viability via influencing membrane physicochemical properties or by facilitating sustained drug release close to its target site of action within the cell (43).

Having confirmed the remarkable cytotoxic effects of VOR-SLNs in three different cell lines, we investigated the oral and IV pharmacokinetic profiles of this formulation in rats. Following oral administration, VOR-SLNs produced significantly higher VOR bioavailability, with a C_{max} and $AUC_{0-\infty}$ that were 1.6- and 2.5-fold higher than those observed following free VOR administration, which clearly indicated the higher GI permeability coefficient and enhanced solubility in GI fluid. Drug-loaded SLNs maintained a higher plasma level at every time point investigated and showed an extended circulation time of up to 24 h, whilst plasma VOR concentration had dropped to below 1 μg/mL by 8 h after administration of the free drug suspension. The high plasma concentration and enhanced bioavailability of VOR delivered in SLNs were attributed to multiple factors: (a) VOR might be well-incorporated into the lipid core of SLN during hot homogenization, providing additional physical stability in the GI and systemic environment, (b) the nano-size of SLN facilitated GI uptake by adhering to the GI tract, (c) the longer chain length of Compritol and the presence of surfactant enhanced VOR-SLNs uptake by lymphatic transport, (d) a well-defined transcellular/paracellular mechanism improved the systemic concentration of drug, and (e) the chylomicrons in the enterocytes played an important role in transporting the intact SLNs (44–46). In addition, SLN components such as Tween

Table IV Pharmacokinetic parameters of VOR after administration of free VOR or VOR-SLNs to rats

Parameters	Oral administration (dose: 30 mg/kg)		IV administration (dose: 10 mg/kg)	
	Free VOR	VOR-SLNs	Free VOR	VOR-SLNs
C_{max} (μg/mL)	8.95 ± 0.12	13.85 ± 3.02*	11.17 ± 0.83	13.00 ± 1.05
$t_{1/2}$ (h)	2.27 ± 1.21	4.94 ± 1.50*	0.65 ± 0.07	4.75 ± 0.90*
$AUC_{0-\infty}$ (μg·h/mL)	27.03 ± 3.25	68.34 ± 13.87*	16.62 ± 1.80	45.45 ± 15.77*
MRT (h)	3.47 ± 1.68	6.92 ± 2.17*	0.77 ± 0.12	5.33 ± 1.07*
T_{max} (h)	1.0 ± 0.0	2.0 ± 0.0	–	–

Data are expressed as the mean ± standard deviation ($n = 4$)

*$p < 0.05$, compared with free VOR

80 and lecithin inhibited the P-gp efflux system, leading to improved oral absorption of VOR (47).

Following IV administration, VOR-SLNs out-performed the free VOR suspension in all pharmacokinetic parameters. The $AUC_{0-\infty}$ of VOR-SLNs was almost 2.7-fold higher than that produced by free VOR, which had disappeared from the blood compartment within 4 h of administration, consistent with its low $t_{1/2}$. These data were consistent with previous reports, which suggested extensive tissue distribution of VOR after IV administration (5). Extensive distribution of VOR may be explained in part by a high tissue uptake because of its high lipid solubility. High distribution of VOR to the liver may also contribute to this, as reported in an earlier study (48). In contrast, incorporation of VOR into the SLN carrier improved drug retention in plasma by 7-fold in rats for up to 24 h. Mean retention time (MRT) is a property of long circulating ability of carrier or drug in the blood compartment. As is seen, SLN formulation increased the MRT of VOR by 2-fold and 6-fold via oral and IV route, respectively. Such an extended plasma $t_{1/2}$ might be attributed to (a) sustained release of VOR from SLNs, as was evident from the *in vitro* release study, and/or (b) surfactants present in the SLN outer layer may provide a hydrophilic shield from RES components such as lipoproteins and opsonin, allowing the SLN to circulate in the blood for longer. This prolonged presence in the systemic circulation should enable SLNs to deliver more entrapped drug to solid tumors, taking advantage of the EPR effect (49–51).

These *in vivo* results clearly showed that SLN had remarkable potential to augment the plasma concentration of VOR. Furthermore, the cytotoxic data showed that VOR-SLN was a more effective cytotoxic agent than free drug in sensitive and drug-resistant cancer cell lines. Taken together, these observations are very significant and meaningful in the context of cancer chemotherapy. A delivery system that can prolong drug $t_{1/2}$ in the systemic circulation and increase its efficacy would markedly enhance its anti-cancer potential and reduce the risk of systemic side effects. This study has provided the first evidence that the physicochemical, pharmacological, and pharmacokinetic properties of VOR can be improved by incorporation into a colloidal lipid carrier.

CONCLUSION

In this study, VOR-SLNs were successfully prepared and optimized to obtain nano-sized particles. SLNs exhibited a high payload capacity for VOR with a sustained release profile. VOR-SLNs were effective in both sensitive and resistant cancer cell lines. Notably, VOR-SLN formulations showed the maximum cytotoxic effect at much lower doses than free VOR in MDA-MB-231 resistant cancer cells, suggesting an ability to effectively counter P-gp related drug efflux pumps. In addition, the cytotoxic effects of VOR-SLNs were more pronounced at longer incubation times, owing to sustained, possibly cytoplasmic, drug release. VOR-SLNs exhibited much higher bioavailability than free VOR in rats, whether administered orally or IV. Taken together, the positive outcomes of this study strongly suggest that delivery using SLN could significantly improve the chemotherapeutic potential of VOR.

ACKNOWLEDGMENTS AND DISCLOSURES

This research was supported by the National Research Foundation of Korea (NRF) grant funded by the Ministry of Education, Science and Technology (No. 2012R1A2A2A02044997 and No. 2012R1A1A1039059).

REFERENCES

1. Marks PA, Breslow R. Dimethyl sulfoxide to vorinostat: development of this histone deacetylase inhibitor as an anticancer drug. Nat Biotechnol. 2007;25:84–90.
2. Cai YY, Yap CW, Wang Z, Ho PC, Chan SY, Ng KY, *et al.* Solubilization of vorinostat by cyclodextrins. J Clin Pharm Ther. 2010;35:521–6.
3. Choo QY, Ho PC, Lin HS. Histone deacetylase inhibitors: new hope for rheumatoid arthritis? Curr Pharm Des. 2008;14:803–20.
4. Bolden JE, Peart MJ, Johnstone RW. Anticancer activities of histone deacetylase inhibitors. Nat Rev Drug Discov. 2006;5:769–84.
5. Mohamed EA, Zhao Y, Meshali MM, Remsberg CM, Borg TM, Foda AM, *et al.* Vorinostat with sustained exposure and high solubility in poly(ethylene glycol)-b-poly(DL-Lactic Acid) micelle nanocarriers: characterization and effects on pharmacokinetics in rat serum and urine. J Pharm Sci. 2012;101:3787–98.
6. Kavanaugh SA, White LA, Kolesar JM. Vorinostat: a novel therapy for the treatment of cutaneous T-cell lymphoma. Am J Health Syst Pharm. 2010;67:793–7.
7. Kelly WK, O'Connor OA, Krug ML, Chiao JH, Heaney M, Curley T, *et al.* Phase I study of an oral histone deacetylase inhibitor, suberoylanilide hydroxamic acid, in patients with advanced cancer. J Clin Oncol. 2005;23:3923–31.
8. Iwamoto M, Friedman EJ, Sandhu P, Agrawal NG, Rubin EH, Wagner JA. Cancer Chemother Pharmacol. 2013;72:493–508.
9. Richard J. Challenges and opportunities in the delivery of cancer therapeutics. Ther Deliv. 2011;2:107–21.
10. Strobl JS, Nikkhah M, Agah M. Actions of the anti-cancer drug suberoylanilide hydroxamic acid (SAHA) on human breast cancer cytoarchitecture in silicon microstructures. Biomaterials. 2010;31:7043–50.
11. Zhang P, Ling G, Pan X, Sun J, Zhang T, Pu X, *et al.* Novel nanostructured lipid-dextran sulfate hybrid carriers overcome tumor multidrug resistance of mitoxantrone hydrochloride. Nanomedicine. 2012;8:185–93.
12. Liu J, Gong T, Wang C, Zhong Z, Zhang Z. Solid lipid nanoparticles loaded with insulin by sodium cholate-phosphatidylcholine-based mixed micelles: preparation and characterization. Int J Pharm. 2007;340:153–62.
13. Das S, Choudhary A. Recent advances in lipid nanoparticle formulations with solid matrix for oral drug delivery. AAPS PharmSciTech. 2011;12:62–76.
14. Suresh G, Manjunath K, Venkateswarlu V, Satyanarayana V. Preparation, characterization, and in vitro and in vivo evaluation of

lovastatin solid lipid nanoparticles. AAPS PharmSciTech. 2007;8:E162–70.
15. Xu Z, Chen L, Gu W, Gao Y, Lin L, Zhang Z, *et al.* The performance of docetaxel-loaded solid lipid nanoparticles targeted to hepatocellular carcinoma. Biomaterials. 2009;30:226–32.
16. Ramasamy TG, Haidar ZS. Formulation, characterization and cytocompatibility evaluation of novel core–shell solid lipid nanoparticles for the controlled and tunable delivery of a model protein. J Bionanosci. 2011;5:143–54.
17. Carneiro G, Silva EL, Pacheco LA, de Souza-Fagundes EM, Corrêa NC, de Goes AM, *et al.* Formation of ion pairing as an alternative to improve encapsulation and anticancer activity of all-trans retinoic acid loaded in solid lipid nanoparticles. Int J Nanomedicine. 2012;7:6011–20.
18. Mussi SV, Silva RC, Oliveira MC, Lucci CM, Azevedo RB, Ferreira LA. New approach to improve encapsulation and antitumor activity of doxorubicin loaded in solid lipid nanoparticles. Eur J Pharm Sci. 2013;48:282–90.
19. Pradhan R, Poudel BK, Ramasamy TG, Choi HG, Yong CS, Kim JO. Docetaxel-loaded PLGA nanoparticles: formulation, physicochemical characterization and cytotoxicity studies. J Nanosci Nanotechnol. 2013;13:5948–56.
20. Marks PA, Dokmanovic M. Histone deacetylase inhibitors: discovery and development as anticancer agents. Expert Opin Investig Drugs. 2005;14:1497–511.
21. Richon VM, Sandhoff TW, Rifkind RA, Marks PA. Histone deacetylase inhibitor selectively induces p21WAF1 expression and gene-associated histone acetylation. Proc Natl Acad Sci U S A. 2000;97:10014–9.
22. Huang JM, Sheard MA, Ji L, Sposto R, Keshelava N. Combination of vorinostat and flavopiridol is selectively cytotoxic to multidrug-resistant neuroblastoma cell lines with mutant TP53. Mol Cancer Ther. 2010;9:3289–301.
23. Ozaki K, Kishikawa F, Tanaka M, Sakamoto T, Tanimura S, Kohno M. Histone deacetylase inhibitors enhance the chemosensitivity of tumor cells with cross-resistance to a wide range of DNA-damaging drugs. Cancer Sci. 2008;99:376–84.
24. Konsoula R, Jung M. In vitro plasma stability, permeability and solubility of mercaptoacetamide histone deacetylase inhibitors. Int J Pharm. 2008;361:19–25.
25. Zhu R, Cheng KW, Mackenzie G, Huang L, Sun Y, Xie G, *et al.* Phospho-Sulindac (OXT-328) Inhibits the Growth of Human Lung Cancer Xenografts in Mice: Enhanced Efficacy and Mitochondria Targeting by its Formulation in Solid Lipid Nanoparticles. Pharm Res. 2012;29:3090–101.
26. Dong X, Mattingly CA, Tseng MT, Cho MJ, Liu Y, Adams VR, *et al.* Doxorubicin and paclitaxel-loaded lipid-based nanoparticles overcome multidrug resistance by inhibiting P-glycoprotein and depleting ATP. Cancer Res. 2009;69:3918–26.
27. Li S, Su Z, Sun M, Xiao Y, Cao F, Huang A, *et al.* Anarginine derivative contained nanostructure lipid carriers with pH-sensitive membranolytic capability for lysosomolytic anti-cancer drug delivery. Int J Pharm. 2012;436:248–57.
28. Chen CC, Tsai TH, Huang ZR, Fang JY. Effects of lipophilic emulsifiers on the oral administration of lovastatin from nanostructured lipid carriers: physicochemical characterization and pharmacokinetics. Eur J Pharm Biopharm. 2010;74:474–82.
29. Kheradmandnia S, Vasheghani-Farahani E, Nosrati M, Atyabi F. Preparation and characterization of ketoprofen-loaded solid lipid nanoparticles made from beeswax and carnauba wax. Nanomedicine. 2010;6:753–9.
30. Lim SJ, Kim CK. Formulation parameters determining the physicochemical characteristics of solid lipid nanoparticles loaded with all-trans retinoic acid. Int J Pharm. 2002;243:135–46.
31. Wissing SA, Müller RH. Solid lipid nanoparticles (SLN)-a novel carrier for UV blockers. Pharmazie. 2001;56:783–6.
32. Venishetty VK, Komuravelli R, Kuncha M, Sistla R, Diwan PV. Increased brain uptake of docetaxel and ketoconazole loaded folate-grafted solid lipid nanoparticles. Nanomedicine. 2013;9:111–21.
33. Yuan H, Miao J, Du YZ, You J, Hu FQ, Zeng S. Cellular uptake of solid lipid nanoparticles and cytotoxicity of encapsulated paclitaxel in A549 cancer cells. Int J Pharm. 2008;348:137–45.
34. Silva AC, Kumar A, Wild W, Ferreira D, Santos D, Forbes B. Long-term stability, biocompatibility and oral delivery potential of risperidone-loaded solid lipid nanoparticles. Int J Pharm. 2012;436:798–805.
35. Kim JO, Ramasamy T, Yong CS, Nukolova N, Bronich TK, Kabanov AV. Cross-linked polymeric micelles based on block ionomer complexes. Mendeleev Comm. 2013;23:179–86.
36. Zhang X, Liu J, Qiao H, Liu H, Ni J, Zhang W, *et al.* Formulation optimization of dihydroartemisinin nanostructured lipid carrier using response surface methodology. Powder Technol. 2010;197:120–8.
37. Rawat K, Jain A, Singh S. Studies on binary lipid matrix based solid lipid nanoparticles of repaglinide: in vitro and in vivo evaluation. J Pharm Sci. 2011;100:2366–78.
38. Muller RH, Radtke M, Wissing SA. Solid lipid nanoparticles (SLN) and nanostructured lipid carriers (NLC) in cosmetic and dermatological preparations. Adv Drug Deliv Rev. 2002;54:S131–55.
39. Bosea S, Duc Y, Takhistovc P, Michniak-Kohn B. Formulation optimization and topical delivery of quercetin from solid lipid based nano systems. Int J Pharm. 2013;441:56–66.
40. Jaina A, Agarwala A, Majumderb S, Lariyaa N, Khayaa A, Agrawalc H, *et al.* Mannosylated solid lipid nanoparticles as vectors for site-specific delivery of an anti-cancer drug. J Control Release. 2010;148:359–67.
41. Gottesman MM, Fojo T, Bates SE. Multidrug resistance in cancer: role of ATP-dependent transporters. Nat Rev Cancer. 2002;2:48–58.
42. Wang S, Chen T, Chen R, Hu Y, Chen M, Wang Y. Emodin loaded solid lipid nanoparticles: preparation, characterization and antitumor activity studies. Int J Pharm. 2012;430:238–46.
43. Di Bernardo G, Alessio N, Dell'Aversana C, Casale F, Teti D, Cipollaro M. Impact of histone deacetylase inhibitors SAHA and MS-275 on DNA repair pathways in human mesenchymal stem cells. J Cell Physiol. 2010;225:537–44.
44. Tiwari R, Pathak K. Nanostructured lipid carrier *versus* solid lipid nanoparticles of simvastatin: comparative analysis of characteristics, pharmacokinetics and tissue uptake. Int J Pharm. 2011;415:232–43.
45. Jacobs C, Kayser O, Muller RH. Nanosuspensions as a new approach for the formulation for the poorly soluble drug tarazepide. Int J Pharm. 2000;196:161–4.
46. Yang S, Zhu J, Lu Y, Liang B, Yang C. Body distribution of camptothecin solid lipid nanoparticles after oral administration. Pharm Res. 1999;16:751–7.
47. Luo YF, Chen DW, Ren LX, Zhao XL, Qin J. Solid lipid nanoparticles for enhancing vinpocetine's oral bioavailability. J Control Release. 2006;114:53–9.
48. Sandhu P, Andrews PA, Baker MP, Koeplinger KA, Soli ED, Miller T, *et al.* Disposition of vorinostat, a novel histone deacetylase inhibitor and anticancer agent, in preclinical species. Drug Metab Lett. 2007;1:153–61.
49. Kim JO, Oberoi H, Desale SH, Kabanov AV, Bronich TK. Polypeptide nanogels with hydrophobic moieties in the cross-linked ionic cores: synthesis, characterization and implications for anticancer drug delivery. J Drug Target. 2013;21:981–93.
50. Tran TH, Ramasamy T, Cho HJ, Kim YI, Poudel BK, Choi HG, *et al.* Formulation and optimization of raloxifene-loaded solid lipid nanoparticles to enhance oral bioavailability. J Nanosci Nanotechnol. 2013;Accepted.
51. Üner M, Yener G. Importance of solid lipid nanoparticles (SLN) in various administration routes and future perspectives. Int J Nanomed. 2007;2:289–300.